Extremophiles (2018) 22:59–71
https://doi.org/10.1007/s00792-017-0977-4

ORIGINAL PAPER

Thermostable and highly specific L-aspartate oxidase from *Thermococcus litoralis* DSM 5473: cloning, overexpression, and enzymological properties

Tsubasa Washio[1] · **Tadao Oikawa**[1,2]

Received: 3 August 2017 / Accepted: 3 November 2017 / Published online: 15 November 2017

Abstract
We successfully expressed the L-aspartate oxidase homolog gene (accession no: OCC_06611) of *Thermococcus litoralis* DSM 5473 in the soluble fraction of *Escherichia coli* BL21 (DE3) using a pET21b vector with 6X His tag at its *C*-terminus. The gene product (*Tl*-LASPO) showed L-aspartate oxidase activity in the presence of FAD in vitro, and this report is the first that details an L-aspartate oxidase derived from a *Thermococcus* species. The homologs of *Tl*-LASPO existed mainly in archaea, especially in the genus of *Thermococcus*, *Pyrococcus*, *Sulfolobus*, and *Halobacteria*. The quaternary structure of *Tl*-LASPO was homotrimeric with a subunit molecular mass of 52 kDa. The enzyme activity of *Tl*-LASPO increased with temperature up to 70 °C. *Tl*-LASPO was active from pH 6.0 to 9.0, and its highest activity was at pH 8.0. *Tl*-LASPO was stable at 80 °C for 1 h. The highest k_{cat}/K_m value was observed in assays at 70 °C. *Tl*-LASPO was highly specific for L-aspartic acid. *Tl*-LASPO utilized fumaric acid, 2,6-dichlorophenolindophenol, and ferricyanide in addition to FAD as a cofactor under anaerobic conditions. The absorption spectrum of holo-*Tl*-LASPO exhibited maxima at 380 and 450 nm. The FAD dissociation constant, K_d, of the FAD-*Tl*-LASPO complex was determined to be 5.9×10^{-9} M.

Keywords *Thermococcus litoralis* · L-Aspartate oxidase · L-Aspartic acid metabolism · Hyperthermophilic archaeon · Thermostable enzyme

Abbreviations

DCIP	2,6-Dichlorophenolindophenol
DTT	Dithiothreitol
DTNB	Dithiobis-(2-nitrobenzoic acid)
EDTA	Ethylenediaminetetraacetic acid
FAD	Flavin adenine dinucleotide
KPB	Potassium phosphate buffer
LB	Luria–Bertani
MALDI-TOF-MS	Matrix-assisted laser desorption–ionization mass spectrometry
NAD	Nicotine adenine dinucleotide
PLP	Pyridoxal 5′-phosphate
PCR	Polymerase chain reaction

Introduction

Thermococcus litoralis DSM 5473 is a hyperthermophilic archaeon and is able to grow under anaerobic conditions at temperatures between 55 and 98 °C, growing optimally at 88 °C (Neuner et al. 1990). In general, enzymes from hyperthermophiles are highly thermostable and have been used for the production of various industrial materials, analytical reagents, and biosensors. The nucleic acid- and carbohydrate-metabolizing enzymes from various strains of *Thermococcus* have been extensively studied. For example, a DNA polymerase (EC 2.7.7.7) from *Thermococcus kodakarensis*, KOD1, is a thermostable and highly accurate enzyme that has been used in PCR (Nishioka et al. 2001). 4-Alpha-glucanotransferase (EC 2.4.1.56) from *T. kodakarensis* catalyzes the intermolecular

Communicated by H. Atomi.

✉ Tadao Oikawa
oikawa@kansai-u.ac.jp

[1] Department of Life Science and Biotechnology, Faculty of Chemistry, Materials and Bioengineering, Kansai University, 3-3-35 Yamate-Cho, Suita, Osaka 564-8680, Japan

[2] Kansai University High Technology Research Center, 3-3-35 Yamate-Cho, Suita, Osaka 564-8680, Japan

transglycosylation of starch and is useful for industrial starch processing (Tachibana et al. 2000).

Amino acid oxidase is an important amino acid-metabolizing enzyme in various organisms and catalyzes the oxidation of amino acids to 2-oxo acids, ammonia, and hydrogen peroxide in the presence of FAD, which is used as a cofactor. Several types of amino acid oxidases, organized by their substrate specificities, have been reported. D-Amino acid oxidase (DAO, EC 1.4.3.3) specifically acts on D-amino acids and has been isolated from *Rhodotorula gracilis* (Pilone et al. 1989), *Arthrobacter protophormia* (Geueke et al. 2007), *Rubrobacter xylanophilus* (Takahashi et al. 2014), and other organisms. The physiological function of DAO is to catabolize D-amino acids in various organisms (Nishikawa 2005). D-Aspartate oxidase (DDO, EC 1.4.3.1) acts mainly on D-aspartic acid and was isolated from *Bos taurus*, *Homo sapiens*, *Octopus vulgaris*, and others. DDO is known to control the D-aspartic acid concentration in mammalian cells (Schell et al. 1997). L-Amino acid oxidase (LAAO, EC 1.4.3.2) acts on various L-amino acids such as L-alanine, L-arginine, L-lysine, L-histidine, and L-leucine and has been isolated from *Crotalus adamanteus* (Wellner and Meister 1960), *Rhizoctonia solani* (Hahn et al. 2017), *Pseudomonas* sp. AIU 813 (Isobe et al. 2012) and others. Snake venom LAAO (and its function) is the most studied LAAO (Mot et al. 2017, Stabeli et al. 2004; Braga et al. 2008; Vargas et al. 2013); the LAAO from king cobra (*Ophiophagus hannah*) venom showed antibacterial activity. L-Glutamate oxidase (LGOX, EC 1.4.3.11) mainly acts on L-glutamic acid and has specifically been isolated from several strains of *Streptomyces,* including *Streptomyces endus* and *Streptomyces violascens*. LGOX is considered to be an important enzyme in L-glutamate metabolism in *Streptomyces* species (Bohmer et al. 1989). L-Aspartate oxidase (LASPO, EC 1.4.3.16) acts mainly on L-aspartate and has been isolated from *Arabidopsis thaliana* (Katoh et al. 2006), *Escherichia coli* (Flachmann et al. 1988), *Sulfolobus tokodaii* (Bifulco et al. 2013), and others. LASPO is physiologically involved in the first reaction of NAD^+ de novo biosynthesis in various organisms. However, studies on LASPO have rarely been compared with those of DDO, DAO, LAAO and LGOX.

We found that an L-aspartate oxidase homolog (OCC_06611) exists in the *T. litoralis* DSM 5473 genome. The gene product of OCC_06611 is expected to be a thermostable L-aspartate oxidase and to be applicable for measurement of L-aspartic acid. In this study, we described the expression of the L-aspartate oxidase homolog gene of *T. litoralis* DSM 5473 in *Escherichia coli* and characterized the enzymological properties of its gene product.

Materials and methods

Materials

Escherichia coli NovaBlue and *Escherichia coli* BL21 (DE3) cells and the pT7blue-2 T-Vector and pET21b vector were purchased from Novagen (Madison, WI, USA). KOD-plus-ver.2 polymerase, DNA ligation kit, and restriction enzymes (*Nde*I and *Xho*I) were purchased from Takara bioscience (Kyoto, Japan). All other reagents were of the best commercially available grade and were purchased from Wako chemicals (Osaka, Japan), Kanto chemicals (Tokyo, Japan), Nacalai tesque (Kyoto, Japan), and Sigma Aldrich (St. Louis, USA).

Cloning and expression of L-aspartate oxidase homolog gene from *Thermococcus litoralis* DSM 5473

The cultivation and genome DNA extraction of *T. litoralis* DSM 5473 were carried out according to the methods that we previously reported (Washio et al. 2016). PCR amplification of the L-aspartate oxidase homolog gene (*Tl-laspo*; accession no. EHR78939) was carried out with a pair of primers [*Tl-laspo* N (with *Nde*I site): TGTTCGGGTAGA CATATGACA, *Tl-laspo* C (with *Xho*I site): CTCGAG TAACATACACCTCCC]. PCR was carried out under the following conditions: polymerase activation at 94 °C for 2 min; denaturation at 98 °C for 30 s; annealing at 55 °C for 30 s; and extension at 68 °C for 90 s. The reaction mixture (total volume: 25 µL) contained 1 × buffer for KOD-plus-ver.2, 0.2 mM dNTP, 1.5 mM $MgSO_4$, primer (*Tl-laspo* N or *Tl-laspo* C (15 pmol)), KOD-plus-ver.2 (1 U), and ultrapure water. PCR products were purified using agarose gel electrophoresis and treated with 10 × A-attachment mix (Toyobo, Osaka, Japan). The reaction product was ligated into a pT7blue2 T-Vector using a Takara DNA ligation kit. The obtained product, the pT7blue2-*Tl-laspo* vector, was transformed into *Escherichia coli* NovaBlue to replicate, and its DNA sequence was analyzed using an Applied Biosystems™ 3130xl DNA analyzer (Applied Biosystems Life Technologies, Foster City, CA, USA). The pT7blue2-*Tl-laspo* vector was digested with *Nde*I and *Xho*I, and the *Tl-laspo* fragment containing *Nde*I and *Xho*I sites was purified

using agarose gel electrophoresis. The *Tl-laspo* fragment that was obtained was ligated to a pET21b vector that had been digested with *Nde*I and *Xho*I. The pET21b-*Tl-laspo* vector that was resulted was transformed into *Escherichia coli* BL21 (DE3). *E. coli* BL21 (DE3) harboring pET21b-*Tl-laspo* was cultivated at 30 °C for 16 h in a test tube (ϕ 18 × 180 mm) containing 5 mL of an LB medium plus 100 μg/mL ampicillin (Medium A) on a reciprocal shaker (Personal-11, Taitec, Saitama, Japan; 140 rpm) under aerobic conditions. Glycerol stocks of *E. coli* BL21 (DE3) harboring pET21b-*Tl-laspo* were prepared by mixing 120 μL of its culture with 30 μL of 80% (w/v) glycerol solution that had been sterilized by autoclave (121 °C, 20 min), and the resulting mixture was stored at − 80 °C.

Purification of recombinant L-aspartate oxidase homolog from *Thermococcus litoralis* DSM 5473

The *Escherichia coli* BL21 (DE3) cells harboring pET21b-*Tl-laspo* were cultivated at 37 °C in four Sakaguchi flasks (500 mL) containing 250 mL of Medium A on a reciprocal shaker under aerobic conditions. After 16 h, the cells were collected by centrifugation at 14,500×*g* and 4 °C for 15 min using an H-923 centrifuge (Kokusan, Tokyo, Japan) and were suspended in 30 mL of 50 mM KPB, pH 7.0, containing 20 mM imidazole and 300 mM NaCl (lysis buffer). This cell suspension was transferred in a conical tube (50 mL) and treated with an ultrasonicator (UD-201, Tomy Seiko, Tokyo, Japan) in ice-cooled water to disrupt the cells (output, 6; duty cycle, 30%). After ultrasonication, the suspension was centrifuged at 14,500×*g* and 4 °C for 20 min. The supernatant was transferred into an Erlenmeyer flask (500 mL) and then incubated with gentle shaking in a water bath at 80 °C. After 15 min, the suspension was centrifuged again under the same conditions to remove insoluble materials, and the supernatant was used as a cell-free extract. The cell-free extract was then applied to a column of Ni–NTA agarose (ϕ 1.5 × 2.8 cm) (Qiagen, Hilden, Germany) that had been equilibrated with lysis buffer. The unabsorbed proteins were washed from the column with a buffer containing 50 mM KPB (pH 7.0), 300 mM NaCl, and 50 mM imidazole. The absorbed protein was eluted with 15 mL of a buffer containing 50 mM KPB (pH 7.0), 300 mM NaCl, and 250 mM imidazole and was stored as a purified enzyme at − 80 °C after it was dialyzed against 50 mM KPB (pH 7.0).

Standard assay conditions

LASPO activity was measured at 70 °C using an assay mixture (3 mL) containing 50 mM KPB, pH 7.0, 50 μM FAD, 2 mM phenol, 0.4 mM 4-aminoantipyrine (4-AA), 30 mM L-aspartic acid, 9.6 U of horseradish peroxidase (HRP, Wako chemical, Osaka, Japan), and enzyme solution. The enzyme reaction was started by the addition of enzyme solution, and the absorption of the solution derived from an oxidative condensation product produced from hydrogen peroxide reacting with the phenol and 4-AA; the absorbance of HRP was measured at 500 nm using a spectrophotometer (JASCO, Tokyo, Japan). One unit of *Tl*-LASPO activity was defined as the amount of enzyme that produces 1 μmol of the oxidative condensation product per minute under standard assay conditions. The molar extinction coefficients (ε_{500}; M^{-1} cm^{-1}) of the oxidative condensation product that were used in various buffers (concentration: 50 mM) were determined experimentally at 70 °C as follows: 7420 in Bis–Tris (pH 6.0); 7440 in Bis–Tris (pH 6.5); 7520 in KPB (pH 6.5); 7600 in KPB (pH 7.0); 7260 in KPB (pH 7.5); 7340 in KPB (pH 8.0); 7300 in Tricine (pH 8.0); 8000 in Tricine (pH 8.5); and 8580 in Tricine (pH 9.0).

Effects of temperature and pH on enzyme activity

The effects of temperature and pH on *Tl*-LASPO activity were examined by measuring the enzyme activity under various temperature and pH conditions. The reaction temperatures were 30, 35, 40, 45, 50, 55, 60, 65, and 70 °C. The buffers were Bis–Tris (pH 6.0 and 6.5); potassium phosphate (pH 6.5, 7.0, 7.5 and 8.0), Tricine–NaOH (pH 8.0, 8.5 and 9.0).

Thermal and pH stability

The pH and thermal stabilities of *Tl*-LASPO were determined by measuring residual activity under the standard assay conditions after pH and heat treatment. The pH treatment was carried out by mixing 100 μL of purified *Tl*-LASPO (0.6 mg/mL) dissolved in 20 mM KPB (pH 7.0) with an equal amount of 250 mM buffer and incubating the solution at 4 °C for 72 h. The buffers were acetate (pH 4.0, 4.5, 5.0, and 5.5); Bis–Tris (pH 5.5, 6.0, and 6.5); potassium phosphate (pH 6.5, 7.0, 7.5, and 8.0); Tricine–NaOH (pH 8.0, 8.5, and 9.0); and glycine–NaOH (pH 9.0, 9.5, and 10.5). The heat treatment was carried out by incubating 500 μL of purified *Tl*-LASPO (4.04 U/mg) dissolved in 20 mM KPB (pH 7.0) at 70, 80, 85, or 90 °C for 0, 10, 20, 30, 40, 50, and 60 min.

Substrate specificity

The substrate specificity of *Tl*-LASPO for various L- and D-amino acids was examined. The tested amino acids used were L-alanine, L-arginine, L-asparagine, L-cysteine,

L-cysteic acid, L-cysteine sulfinic acid, L-glutamate, L-glutamine, L-histidine, L-isoleucine, L-leucine, L-lysine, L-methionine L-phenylalanine, L-proline, L-serine, L-threonine, L-tryptophan, L-tyrosine, L-valine, glycine, D-asparagine, D-aspartate, and D-glutamate. Each amino acid replaced L-aspartic acid in the standard assay mixture at a final concentration of 30 mM except for L-tyrosine (final conc. 5 mM), and the enzyme activity was measured under standard assay conditions.

Tl-LASPO specificity for electron acceptor

The specificity of *Tl*-LASPO for electron acceptor was examined by testing fumaric acid, 2,6-dichlorophenolindophenol (DCIP), and ferricyanide as acceptors. The enzyme reaction was carried out anaerobically at 70 °C in a glove box (As one, Osaka, Japan) that had been filled with argon gas (purity: 99.99%). The reaction mixture (total volume: 0.3 mL) contained 50 mM KPB (pH 7.0), 50 μM FAD, 30 mM L-aspartic acid, and purified *Tl*-LASPO (28 μg), and 30 mM fumaric acid, 42 μM DCIP or 1 mM ferricyanide was added as an electron acceptor. The reaction was stopped by the addition of 60% (w/w) perchloric acid (for fumaric acid) or 10% SDS (w/v) (for DCIP and ferricyanide). In experiments with fumaric acid, the ammonium that was produced in the solution was quantified using Nessler's reagent. An aliquot of the solution (10 μL) was mixed with Nessler's reagent (10 μL) and deionized water (180 μL), and the absorption of the resulting solution was measured at 450 nm. The amount of ammonium was determined based on the calibration curve that was generated using ammonium sulfate as a standard. One unit of *Tl*-LASPO activity was defined as the amount of enzyme that produces 1 μmol of NH_4^+ per minute. In experiments with DCIP or ferricyanide, the absorption changes were measured at 600 nm for DCIP (ε_{600} was calculated to be 17,970 M^{-1} cm^{-1}) and at 420 nm for ferricyanide (ε_{420} = 970 M^{-1} cm^{-1}). One unit of *Tl*-LASPO activity was defined the amount of enzyme that produces 1 μmol of the reduced form of DCIP or ferricyanide per minute at 70 °C.

Kinetic analysis

Tl-LASPO activities were measured with various concentrations of L-aspartic acid (5, 10, 15, 30 and 60 mM) at 37, 50, 60, and 70 °C under standard assay conditions. The kinetic parameters (K_m and k_{cat}) of the reaction of *Tl*-LASPO with L-aspartic acid were determined by analyzing the enzyme activities at each reaction temperature with a Lineweaver–Burk plot (Lineweaver and Burk 1934).

Molecular mass and quaternary structure

The subunit molecular mass of *Tl*-LASPO was determined using SDS-PAGE with a 12% T or 10% T polyacrylamide gel. The purified *Tl*-LASPO (50 μL) was mixed with 2 × sample buffer (50 μL) containing 125 mM Tris–HCl buffer (pH 6.8), 4% (w/v) SDS, 10% (w/v) sucrose, 0.01% bromophenol blue, and 5 or 0.05% (v/v) 2-mercaptoethanol, and the sample was then incubated at 100 °C for 5 min.

The molecular mass of purified *Tl*-LASPO was estimated by gel filtration. The standard proteins were apoferritin (443 kDa), β-amylase (200 kDa), albumin (66 kDa), carbonic anhydrase (29 kDa), and cytochrome *c* (12.4 kDa). The standard proteins (1.0 mg) were dissolved in 0.1 mL of 50 mM KPB (pH 7.0) and this solution was applied to a column of Superdex 200 (ϕ 10 × 300 cm, GE Healthcare, Tokyo, Japan) that had been equilibrated with 50 mM KPB (pH 7.0) containing 150 mM NaCl. The column was eluted with the same buffer at a flow rate of 0.5 mL/min. After the standard calibration curve had been prepared, purified *Tl*-LASPO (2.0 mg/mL, 0.1 mL) was applied to the column under the same conditions.

Spectral analysis of holo- and apoenzyme

The *Tl*-LASPO apoprotein was prepared by dialyzing the holoprotein of *Tl*-LASPO (approximately 10 mg) against 500 mL of 50 mM KPB (pH 7.0) containing 3 M KBr and 0.5% (w/v) charcoal at 4 °C for 72 h. The dialysis buffer was changed after 24 and 48 h. After 72 h, the dialysate was corrected and applied to a column of PD-10 (GE Healthcare, Piscataway, NJ, USA) equilibrated with 50 mM KPB (pH 7.0). The UV–VIS spectra of the *Tl*-LASPO holo- and apoproteins were measured using a spectrophotometer (JASCO, Tokyo, Japan). The sample was diluted with 50 mM KPB (pH 7.0) to a concentration of 1.4 mg/mL.

Determination of FAD dissociation constant

The FAD dissociation constant (K_d) of the FAD-*Tl*-LASPO complex was determined by measuring the quenching of FAD fluorescence that occurred when apo-*Tl*-LASPO was titrated with FAD. FAD fluorescence was measured using a Hitachi F-2500 spectrofluorometer (Hitachi High-Technologies, Tokyo, Japan). The measurement conditions were excitation wavelength (slit width, 10 nm) 450 nm and emission wavelength (slit width, 20 nm) 522.5 nm. Apo-*Tl*-LASPO was diluted with 50 mM KPB, pH 7.0, to a final concentration of 7.0 μM, and the FAD concentration was varied from 0 to 24.5 μM

using a 50 μM FAD (dissolved in water) stock solution. The K_d value was calculated according to the method of Arroyo et al. (2007) using Eq. (1):

$$1/(1-a) = 1/K_d([L_0]/a - [E_0]). \quad (1)$$

The parameters in Eq. (1) were as follows: a is the fractional saturation of total concentration of binding site; K_d is the dissociation constant; $[L_0]$ is the total ligand concentration; and $[E_0]$ is the total enzyme concentration.

MALDI-TOF-MS analysis

The protein band that had been removed from a SDS-polyacrylamide gel was cut into small pieces (approximately 1 × 1 mm). The gel pieces were put into a microcentrifuge tube and treated with an In-Gel Tryptic Digestion Kit (Thermo Fisher Scientific, Yokohama, Japan) according to its manufacturer's instructions. The sample that had been digested with trypsin was desalted using a Zip Tip C18 (Millipore, Billerica, MA, USA). The desalted sample (0.5 μL) was mixed with 0.5 μL of matrix solution (2,5-dihydroxybenzoic acid dissolved at a concentration of 1 mg/mL in ultrapure deionized water) containing 40% (v/v) acetonitrile and 0.06% (v/v) trifluoroacetic acid and was put on a MALDI target plate. After the sample was dried naturally with air, mass spectrometry measurements were carried out in reflectron positive ion mode using an AXIMA-CFR-plus MALDI-TOF-MS instrument (Shimadzu, Kyoto, Japan). The mass spectrometry data were analyzed using MASCOT (Matrix science, London, UK) to identify the trypsin-digested peptides and comparing them with peptide sequences in protein databases.

Effects of pH on thiol oxidation during storage of purified enzyme

The purified *Tl*-LASPO, dissolved in 50 mM KPB, pH 7.0 (2 mL), was passed through a PD-10 (GE Healthcare Japan, Tokyo, Japan) column that had been equilibrated with various buffers (50 mM Bis–Tris, pH 6.0; 50 mM sodium phosphate buffer, pH 7.0 and 8.0; or glycine–NaOH, pH 9.0) to exchange the sample buffer, and the resulting solution was stored at 4 °C. After 168 h had passed, the free thiol content in *Tl*-LASPO was quantitated using DTNB (Patsoukis and Georgiou, 2004). The sample (30 μL) was mixed with 500 mM sodium phosphate buffer, pH 8.0 (60 μL), 25 mM EDTA (6 μL), and 10 mM DTNB (24 μL), and the solution was allowed to react at 25 °C for 40 min. The absorption of the sample was measured at 412 nm, and the concentration of free thiol groups was determined according to the calibration curve that had been constructed using reduced glutathione (conc.: 0, 5, 10, 20, and 40 μM) as a standard.

Phylogenetic analysis

To clarify the distribution of homologs of *Tl*-LASPO, we performed the phylogenetic analysis with 71 kinds of the primary structure of L-aspartate oxidase registered already in protein data bank of BLAST program according to the method of Altschul et al. (1990). The phylogenetic tree of L-aspartate oxidase was described using a Clustal W multiple sequence alignment with a MEGA4 program (Thompson et al. 2002) by the method of neighbor-joining (Saitou and Nei 1987).

Accession numbers

The accession number of gene or protein written in this paper was expressed as the number administrated in National Center for Biotechnology Information (NCBI; https://www.ncbi.nlm.nih.gov), and the Reference Sequence (RefSeq) number of NCBI was used only for the protein without accession number.

Results

Expression of L-aspartate oxidase homolog gene from *Thermococcus litoralis* DSM 5473 and purification and characterization of its gene product

DNA sequence analysis showed that the *Tl-laspo* gene was composed of 1398 bp and encoded 465 amino acid residues. Genes encoding homologs of quinolinate synthetase (EC 2.5.1.72) and nicotinate nucleotide pyrophosphorylase (EC 2.4.2.19) were downstream of the *Tl-laspo* gene, while two genes encoding hypothetical proteins were upstream. The amino acid sequence of *Tl*-LASPO was similar to those of other previously reported L-aspartate oxidases, and its similarity to amino acid sequences of LASPOs from *Pyrococcus horikoshii* OT-3, *Sulfolobus tokodaii* 7, *Bacillus subtilis* 168, and *Escherichia coli* K-12 was calculated to be approximately 65, 38, 35 and 34%, respectively (Fig. 1). The important amino acid residues in the putative FAD binding site were well conserved in the primary structure of *Tl*-LASPO: Ala12, Gln43, Gly45, Glu331, and Leu348 (Fig. 1). The phylogenetic analysis of L-aspartate oxidase revealed that the homologs of *Tl*-LASPO existed in three of ten classes of archaea, *Thermococci*, *Thermoprotei*, and *Halobacteria*, especially in the genus of *Thermococcus*,

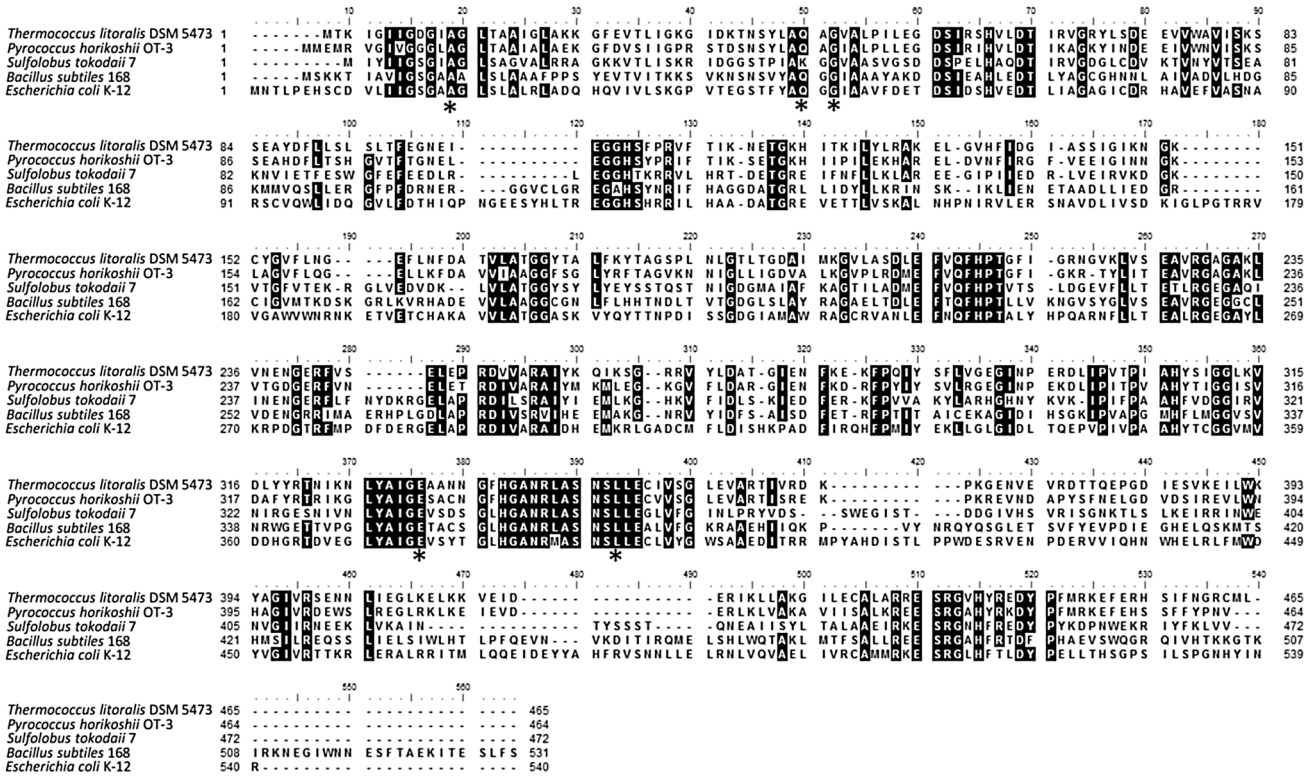

Fig. 1 Alignment of amino acid sequences of L-aspartate oxidases from *Thermococcus litoralis* DSM 5473 and other microorganisms. Asterisk conserved amino acid residues for FAD binding. The amino acid sequences used for alignment were as follows: *Thermococcus litoralis* DSM 5473 (accession no.: EHR78939), *Pyrococcus horikoshii* OT-3 (accession no.: BAA29083), *Sulfolobus tokodaii* 7 (accession no.: BAK54476), *Bacillus subtilis* 168 (accession no.: AIY94113), and *Escherichia coli* K-12 (accession no.: AMH35960)

Pyrococcus, *Sulfolobus*, and *Halobacteria* that belong to the families of *Thermococcaceae*, *Sulfobaceae*, or *Halobacteriaceae* (Fig. 2). In domain of Bactria, the homologs of *Tl*-LASPO existed predominantly in the family of *Aquificaceae* (Fig. 2), although LASPO was purified from several bacteria such as *Escherichia coli* (Flachmann et al. 1988), *Bacillus subtilis* (Marinoni et al. 2008), *Pseudomonas putida* (Leese et al. 2013), and so on. *Tl*-LASPO was also homologous to the proteins that were annotated as a fumarate reductase in some archaea (Fig. 2).

We succeeded in expressing *Tl*-LASPO in soluble fractions of *E. coli* BL21 (DE3) cells harboring pET21b-*Tl-laspo* cells. Approximately, 60% of the *Tl*-LASPO protein was detected in soluble fractions using SDS-PAGE analysis. *Tl*-LASPO was purified to homogeneity from cell-free extracts of *E. coli* BL21 (DE3) cells harboring pET21b-*Tl-laspo* using heat treatment and Ni–NTA and hydroxyapatite columns (Fig. 3), and approximately 20 mg of purified *Tl*-LASPO was obtained from cell-free extracts that were prepared from 1 L of culture. The specific activity of purified *Tl*-LASPO was 3.86 U/mg. The molecular mass of the *Tl*-LASPO was calculated to be approximately 140 kDa by gel-filtration (Fig. 3c). The subunit molecular mass of *Tl*-LASPO was calculated to be approximately 52 kDa by SDS-PAGE. Accordingly, the quaternary structure of *Tl*-LASPO was determined to be homotrimeric. We found that after storage of the purified *Tl*-LASPO at 4 °C for more than 96 h, a protein band corresponding to a molecular mass of 100 kDa, in addition to the band at 52 kDa, appeared in SDS-PAGE analysis (Fig. 3a); however, the specific activity of the purified *Tl*-LASPO did not change during the storage period. The MALDI-TOF-MS analysis showed that the protein bands at both 52 and 100 kDa were derived from the polypeptide chain of *Tl*-LASPO and did not contain peptides from other proteins (Table 1). We examined the effects of storage pH (pH 6–9) on the appearance of the protein band of 52 kDa and found that the intensity of the protein band gradually increased at acidic pH values and peaked at pH 6.0 (Fig. 3b). The number of free thiol groups in purified *Tl*-LASPO during storage also decreased at acidic pH and was lowest at pH 6.0 (Table 2). These results suggested that the protein band at 100 kDa might be composed of two polypeptide chains of *Tl*-LASPO.

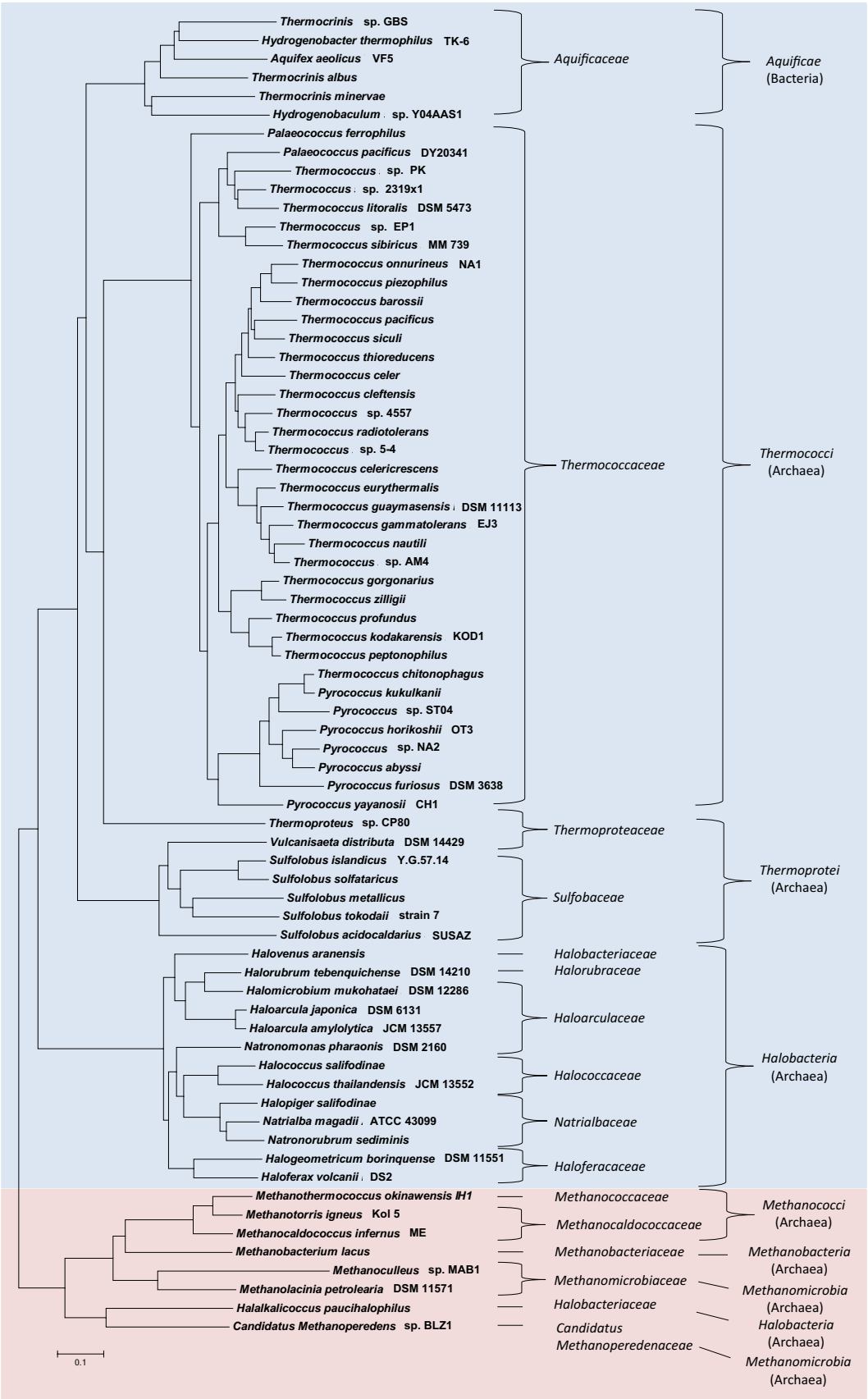
Thermocrinis sp. GBS
Hydrogenobacter thermophilus TK-6
Aquifex aeolicus VF5
Thermocrinis albus
Thermocrinis minervae
Hydrogenobaculum sp. Y04AAS1
Aquificaceae
Aquificae (Bacteria)
Palaeococcus ferrophilus
Palaeococcus pacificus DY20341
Thermococcus sp. PK
Thermococcus sp. 2319x1
Thermococcus litoralis DSM 5473
Thermococcus sp. EP1
Thermococcus sibiricus MM 739
Thermococcus onnurineus NA1
Thermococcus piezophilus
Thermococcus barossii
Thermococcus pacificus
Thermococcus siculi
Thermococcus thioreducens
Thermococcus celer
Thermococcus cleftensis
Thermococcus sp. 4557
Thermococcus radiotolerans
Thermococcus sp. 5-4
Thermococcus celericrescens
Thermococcus eurythermalis
Thermococcus guaymasensis DSM 11113
Thermococcus gammatolerans EJ3
Thermococcus nautili
Thermococcus sp. AM4
Thermococcus gorgonarius
Thermococcus zilligii
Thermococcus profundus
Thermococcus kodakarensis KOD1
Thermococcus peptonophilus
Thermococcus chitonophagus
Pyrococcus kukulkanii
Pyrococcus sp. ST04
Pyrococcus horikoshii OT3
Pyrococcus sp. NA2
Pyrococcus abyssi
Pyrococcus furiosus DSM 3638
Pyrococcus yayanosii CH1
Thermococcaceae
Thermococci (Archaea)
Thermoproteus sp. CP80
Vulcanisaeta distributa DSM 14429
Thermoproteaceae
Sulfolobus islandicus Y.G.57.14
Sulfolobus solfataricus
Sulfolobus metallicus
Sulfolobus tokodaii strain 7
Sulfolobus acidocaldarius SUSAZ
Sulfobaceae
Thermoprotei (Archaea)
Halovenus aranensis
Halobacteriaceae
Halorubrum tebenquichense DSM 14210
Halorubraceae
Halomicrobium mukohataei DSM 12286
Haloarcula japonica DSM 6131
Haloarcula amylolytica JCM 13557
Haloarculaceae
Natronomonas pharaonis DSM 2160
Halococcus salifodinae
Halococcus thailandensis JCM 13552
Halococcaceae
Halopiger salifodinae
Natrialba magadii ATCC 43099
Natronorubrum sediminis
Natrialbaceae
Halogeometricum borinquense DSM 11551
Haloferax volcanii DS2
Haloferacaceae
Halobacteria (Archaea)
Methanothermococcus okinawensis IH1
Methanococcaceae
Methanotorris igneus Kol 5
Methanocaldococcaceae
Methanocaldococcus infernus ME
Methanococci (Archaea)
Methanobacterium lacus
Methanobacteriaceae
Methanobacteria (Archaea)
Methanoculleus sp. MAB1
Methanolacinia petrolearia DSM 11571
Methanomicrobiaceae
Methanomicrobia (Archaea)
Halalkalicoccus paucihalophilus
Halobacteriaceae
Halobacteria (Archaea)
Candidatus Methanoperedens sp. BLZ1
Candidatus Methanoperedenaceae
Methanomicrobia (Archaea)
0.1

◂**Fig. 2** Phylogenetic analysis of L-aspartate oxidase from *Thermococcus litoralis* DSM 5473. The blue colored area showed the proteins annotated as L-aspartate oxidase and the pink colored area showed the proteins annotated as fumarate reductase. The amino acid sequences used for phylogenetic analysis were shown as follows: *Aquifex aeolicus* VF5 (accession no.: AAC06932), *Candidatus Methanoperedens* sp. BLZ1 (accession no.: KPQ41658), *Halalkalicoccus paucihalophilus* (accession no.: KYH26718), *Haloarcula amylolytica* JCM 13557 (accession no.: EMA20236), *Halococcus salifodinae* (accession no.: EMA49854), *Halococcus thailandensis* JCM 13552 (accession no.: EMA50543), *Haloferax volcanii* DS2 (accession no.: ADE03658), *Halogeometricum borinquense* DSM 11551 (accession no.: ADQ66598), *Halomicrobium mukohataei* DSM 12286 (accession no.: ACV47611), *Halopiger salifodinae* (accession no.: SEW21219), *Halorubrum tebenquichense* DSM 14210 (accession no.: ELZ40236), *Halovenus aranensis* (accession no.: SDJ44082), *Hydrogenobacter thermophilus* TK-6 (accession no.: BAI68789), *Hydrogenobaculum* sp. Y04AAS1 (accession no.: ACG57280), *Methanobacterium lacus* (accession no.: ADZ08296), *Methanocaldococcus infernus* ME (accession no.: ADG13203), *Methanoculleus* sp. MAB1 (accession no.: CVK31361), *Methanolacinia petrolearia* DSM 11571 (accession no.: ADN37392), *Methanothermococcus okinawensis* IH1 (accession no.: AEH06252), *Methanotorris igneus* Kol 5 (accession no.: AEF95579), *Natrialba magadii* ATCC 43099 (accession no.: ADD06474), *Natronomonas pharaonis* DSM 2160 (accession no.: CAI49299), *Natronorubrum sediminis* (accession no.: SEH16664), *Palaeococcus ferrophilus* (RefSeq no.: WP_048149971), *Palaeococcus pacificus* DY20341 (accession no.: AIF68566), *Pyrococcus abyssi* (RefSeq no.: WP_048147208), *Pyrococcus furiosus* DSM 3638 (accession no.: AAL82100), *Pyrococcus horikoshii* OT3 (accession no.: BAA29083), *Pyrococcus kukulkanii* (accession no.: AMM54247), *Pyrococcus* sp. NA2 (accession no.: AEC51452), *Pyrococcus* sp. ST04 (accession no.: AFK21679), *Pyrococcus yayanosii* CH1 (accession no.: AEH25409), *Sulfolobus acidocaldarius* SUSAZ (accession no.: AHC50960), *Sulfolobus islandicus* Y.G.57.14 (accession no.: ACP45480), *Sulfolobus metallicus* (RefSeq no.: WP_054839231), *Sulfolobus solfataricus* 98/2 (accession no.: AKA74220), *Sulfolobus tokodaii* 7 (accession no.: BAK54476), *Thermococcus barossii* (accession no.: ASJ03836), *Thermococcus celer* (accession no.: ASI98302), *Thermococcus celericrescens* (accession no.: KUH32063), *Thermococcus chitonophagus* (accession no.: ASJ15662), *Thermococcus cleftensis* (accession no.: AFL95005), *Thermococcus eurythermalis* (accession no.: AIU68991), *Thermococcus gammatolerans* EJ3 (accession no.: ACS33122), *Thermococcus gorgonarius* (accession no.: ASJ01095), *Thermococcus guaymasensis* DSM 11113 (accession no.: AJC71951), *Thermococcus kodakarensis* KOD1 (accession no.: BAD84486), *Thermococcus litoralis* DSM 5473 (accession no.: EHR78939), *Thermococcus nautili* (accession no.: AHL22922), *Thermococcus onnurineus* NA1 (accession no.: ACJ17376), *Thermococcus pacificus* (accession no.: ASJ06406), *Thermococcus peptonophilus* (accession no.: AMQ18168), *Thermococcus piezophilus* (accession no.: ANF22655), *Thermococcus profundus* (accession no.: ASJ03423), *Thermococcus radiotolerans* (accession no.: ASJ15399), *Thermococcus sibiricus* MM 739 (accession no.: ACS89124), *Thermococcus siculi* (accession no.: ASJ08395), *Thermococcus* sp. 2319 × 1 (accession no.: ALV63936), *Thermococcus* sp. 4557 (accession no.: AEK73068), *Thermococcus* sp. 5-4 (accession no.: ASA76763), *Thermococcus* sp. AM4 (accession no.: EEB74599), *Thermococcus* sp. EP1 (accession no.: KPU63813), *Thermococcus* sp. PK (RefSeq no.: WP_083965087), *Thermococcus thioreducens* (accession no.: ASJ11607), *Thermococcus zilligii* (RefSeq no.: WP_010478909), *Thermocrinis albus* (RefSeq no.: WP_041434046), *Thermocrinis minervae* (accession no.: SHK43562), *Thermocrinis* sp. GBS (RefSeq no.: WP_029551840), *Thermoproteus* sp. CP80 (RefSeq no.: WP_081226661), *Vulcanisaeta distributa* DSM 14429 (accession no.: ADN49891)

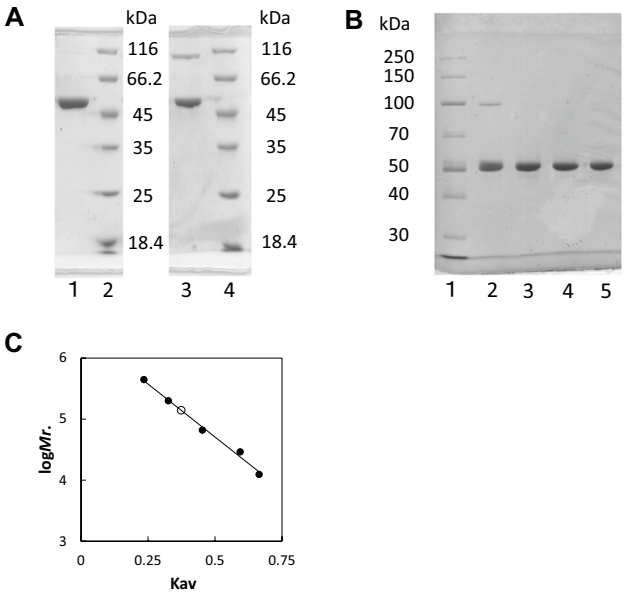

Fig. 3 Molecular mass and subunit molecular mass of purified L-aspartate oxidase from *Thermococcus litoralis* DSM 5473. **a** Effects of storage time on the appearance of 100-kDa band. Lanes 1, 3: 5 µg of purified *Tl*-LASPO stored at 4 °C for 0 and 192 h, respectively. Lanes 2,4: Molecular mass marker (4 µL): 14.4 kDa (Lysozyme), 18.4 kDa (β-Lactoglobulin), 25.0 kDa (REase Bsp98 I), 35.0 kDa (Lactate dehydrogenase), 45.0 kDa (Ovalbumin), 66.2 kDa (Bovine serum albumin), and 116 kDa (β-Galactosidase). SDS-PAGE was carried out using 12%T polyacrylamide gels. The samples were treated with sample buffer containing 5% 2-mercaptoethanol. **b** Effects of storage pH on the appearance of 100-kDa band. Lane 1: molecular mass marker (4 µL). PageRuler™ Unstained Broad Range Protein Ladder (Thermo fisher scientific, Waltham, MA, USA). Lanes 2, 3, 4, 5: 5 µg of purified *Tl*-LASPO stored at various pH values (lane 2, pH 6.0; lane 3, pH 7.0; lane 4, pH 8.0; and lane 5, pH 9.0). SDS-PAGE was carried out using 10%T polyacrylamide gels. The samples were treated with sample buffer containing 0.05% 2-mercaptoethanol. **c** Molecular mass. Filled circle: standard proteins, open circle: *Tl*-LASPO. 12.4 kDa (Cytochrome *c*), 29 kDa (Carbonic anhydrase), 66 kDa (Albumin), 200 kDa (β-Amylase), and 443 kDa (Apoferritin)

Effects of pH and temperature on the activity of the L-aspartate oxidase from *Thermococcus litoralis* DSM 5473

The enzyme activity of *Tl*-LASPO increased as the reaction temperature increased from 30 to 70 °C (Fig. 4a). The enzyme activity of *Tl*-LASPO was measured from pH 6.0 to 9.0, and it peaked at pH 8.0 when a potassium phosphate buffer was used in the assay (Fig. 4b). *Tl*-LASPO was stable at temperatures up to 80 °C when heat treated for 1 h (Fig. 5a). The half-life time of *Tl*-LASPO at 90 and 85 °C was calculated to be 46 and 170 min, respectively. Approximately, 70% of its initial activity remained after being incubated at 85 °C for 1 h. The thermal stability

Table 1 MALDI-TOF/MS analysis

Mass value	Position	The band of 52 kDa (monomeric *Tl*-LASPO)		The band of 100 kDa		Sequence
		Observed mass value	M.C.	Observed mass value	M.C.	
3103.30	83–110	3101.56	0	n.d.		SSEAYDFLLSLSLTFEGNEIEGGHSFPR
3032.39	152–179	n.d.		n.d.		CYGVFLNGEFLNFDATVLATGGYTALFK
2190.45	199–218	n.d.		2189.50	0	GVLASDLEFVQFHPTGFIGR
2188.45	37–57	2188.63	0	2188.05	0	TNSYLAQAGVALPILEGDSIR
1966.18	281–297	1965.64	0	1965.12	0	FPQIYSFLVGEGINPER
1923.19	180–198	1922.63	0	n.d.		YTAGSPLNLGTLTGDAIMK
1888.99	325–342	1888.56	0	1888.11	0	NLYAIGEAANNGFHGANR
1874.18	343–360	n.d.		n.d.		LASNSLLECIVSGLEVAR
1794.10	298–314	1793.71	0	1793.30	0	DLIPVTPIAHYSIGGLK
1756.02	132–148	1755.69	0	1755.29	0	ELGVHFIDGIASSIGIK
1724.07	4–22	1723.77	0	1723.34	0	IGIIGDGIAGLTAAIGLAK
1637.82	69–82	1637.64	0	1637.26	0	YLSDEEVVWAVISK
1428.45	376–388	1418.59	0	1418.28	0	DTTQEPGDIESVK
1369.51	267–278	1369.63	0	n.d.		VYLDATGIENFK
1116.22	400–409	1116.60	0	1116.32	0	SENNLIEGLK
976.08	243–250	976.55	0	976.30	0	FVSELEPR
963.12	24–32	963.55	0	n.d.		GFEVTLIGK
957.06	444–450	957.47	0	957.21	0	EDYPFMR
945.15	426–434	945.56	0	n.d.		GILECALAR
940.07	58–65	940.57	0	940.33	0	SHVLDTIR
929.97	235–242	930.51	0	930.27	0	LVNENGER
829.91	456–462	830.48	0	830.26	0	HSIFNGR
827.93	315–320	828.48	0	828.27	0	VDLYYR
801.84	369–375	802.47	0	802.24	0	GENVEVR
772.90	223–229	773.51	0	773.30	0	LVSEAVR
759.81	414–419	760.46	0	n.d.		VEIDER
606.75	111–115	n.d.		608.18	0	VFTIK

n.d. not detected, *M.C.* number of miss cleavages

Table 2 Measurement of free thiol group

Storage pH	Thiol groups concentration (μM)
6.0	3.9 ± 1.1
7.0	8.6 ± 2.0
8.0	14.8 ± 3.1
9.0	16.0 ± 0.9

($n = 3$)

of *Tl*-LASPO was similar to that of other LASPOs from hyperthermophiles such as *Sulfolobus tokodaii* (stable up to 80 °C) (Sakuraba et al. 2008) and *Pyrococcus horikoshii* (high stability at 80 °C) (Sakuraba et al. 2002). *Tl*-LASPO was highly stable between pH 5.0 and 10.5 (Fig. 5b).

Substrate specificity

Tl-LASPO was highly specific for L-aspartic acid and did not act on other natural amino acids, although it showed weak activity against the unnatural amino acids L-cysteic acid (relative activity to L-aspartic acid: 4.02%) and L-cysteine sulfinic acid (1.09%) (Table 3). Compared with *Tl*-LASPO, the LASPOs from other microorganisms showed relatively low substrate specificity: the *Sulfolobus tokodaii* strain 7 enzyme acted on L-aspartic acid and L-asparagine (Bifulco et al. 2013), and the *Pseudomonas putida* ATCC 47054 enzyme acted on L-asparagine and L-glutamate (Leese et al. 2013).

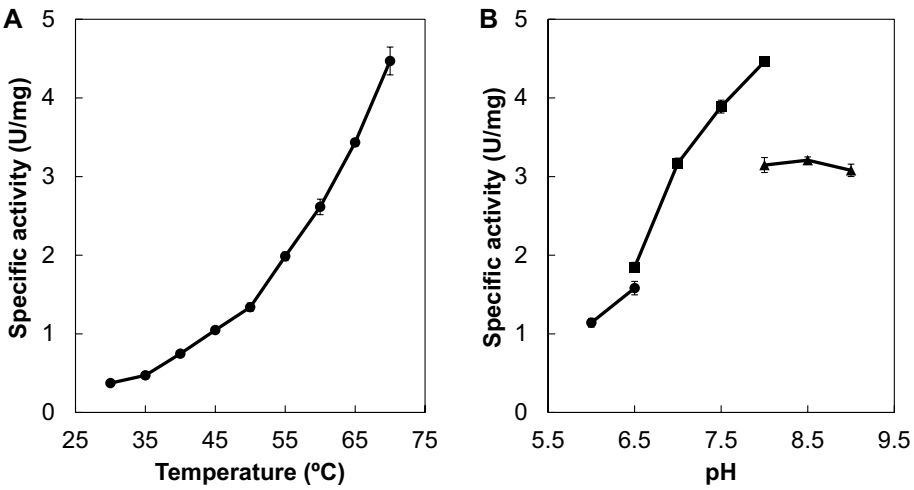

Fig. 4 Effects of temperature and pH on the activity of the L-aspartate oxidase from *Thermococcus litoralis* DSM 5473. **a** Effect of temperature. **b** Effect of pH. Filled circles, Bis–Tris pH 6.0–6.5; filled squares, potassium phosphate, pH 6.5–8.0; filled triangles, Tricine–NaOH pH 8.0–9.0

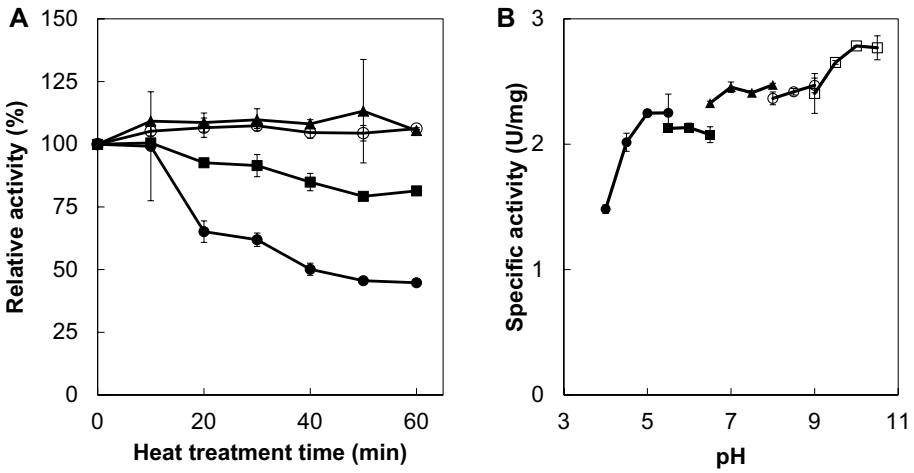

Fig. 5 Thermal and pH stability of the L-aspartate oxidase from *Thermococcus litoralis* DSM 5473. **a** Thermal stability. Filled circles, 90 °C; filled squares, 85 °C; filled triangles, 80 °C; and open circles, 70 °C. **b** pH stability of *Tl*-LASPO. Filled circles, sodium acetate pH 4.5–5.5; filled squares, Bis–Tris pH 5.5–6.5; filled triangles, potassium phosphate pH 6.5–8.0; open circles, Tricine–NaOH pH 8.0–9.0; open squares, glycine–NaOH pH 9.0–10.5

Tl-LASPO specificity for electron acceptor

Tl-LASPO utilized fumaric acid, DCIP, and ferricyanide individually as cofactors under anaerobic conditions. The specific activities were calculated to be 0.96 ± 0.02, 3.7 ± 0.6, and 15.7 ± 1.2 U/mg for fumaric acid, DCIP, and ferricyanide, respectively.

Kinetic parameters

The kinetic parameters describing *Tl*-LASPO activity are summarized in Table 4. The K_m value for L-aspartic acid decreased with increasing reaction temperature, while the k_{cat} value increased; the highest catalytic efficiency of *Tl*-LASPO, i.e., k_{cat}/K_m value, in the temperature range tested was observed in the assays at 70 °C. The K_m value of *Tl*-LASPO activity for L-aspartic acid at 37 °C was higher than that of the enzyme from *S. tokodaii* strain 7 (13.3 mM, at 37 °C, pH 8.0) (Bifulco et al. 2013). Accordingly, *Tl*-LASPO showed the lower affinity to L-aspartic acid under low temperature conditions as compared with the enzyme from *S. tokodaii* strain 7.

Spectroscopic properties, FAD content, and FAD dissociation constant

FAD bound tightly to *Tl*-LASPO and did not dissociate when treated with 3 M KBr. In addition to KBr, we used charcoal and succeeded in preparing apo-*Tl*-LASPO. The absorption spectrum of holo-*Tl*-LASPO showed maxima at 380 and 450 nm, and these peaks were not present in apoenzyme (Fig. 6). Titrating apo-*Tl*-LASPO with FAD exhibited fluorescence at 522.5 nm that demonstrated a break point at 1 mol of FAD/mol of subunit (Fig. 7). Accordingly, the spectral features of holo-*Tl*-LASPO were derived from FAD, and *Tl*-LASPO contained 1 mol of FAD per subunit. The FAD

Table 3 Substrate specificity

Substrate	Specific activity (U/mg)
L-Aspartic acid	3.69 ± 0.19
D-Aspartic acid	0
L-Cysteinic acid	0.15 ± 0.01
L-Cysteinesulfinic acid	0.04 ± 0.00
L-Asparagine	0
D-Asparagine	0
L-Glutamic acid	0
D-Glutamic acid	0
L-Glutamine	0
L-Alanine	0
L-Valine	0
L-Leucine	0
L-Isoleucine	0
L-Proline	0
L-Serine	0
L-Threonine	0
L-Methionine	0
L-Cysteine	0
L-Histidine	0
L-Arginine	0
L-Lysine	0
L-Phenylalanine	0
L-Tryptophan	0
L-Tyrosine	0
Glycine	0

($n = 3$)

dissociation constant, K_d, of the FAD-*Tl*-LASPO complex was calculated to be 5.6×10^{-9} M.

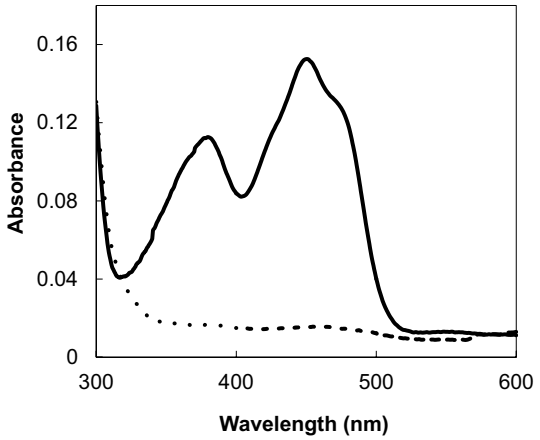

Fig. 6 Spectral analysis of holo- and apo-L-aspartate oxidase from *Thermococcus litoralis* DSM 5473. Solid line, holoprotein; dashed line, apoprotein. Protein concentration: 22.5 µM. Buffer: 50 mM KPB (pH 7.0)

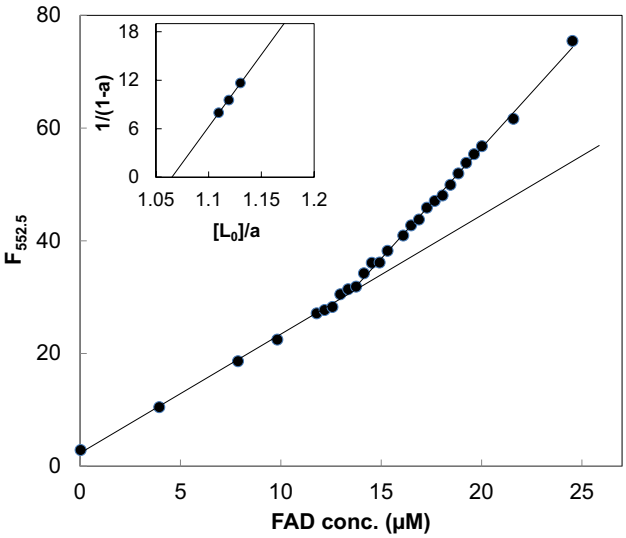

Fig. 7 Determination of dissociation constant of FAD/L-aspartate oxidase from *Thermococcus litoralis* DSM 5473 complex

Discussion

We succeeded in expressing an L-aspartate oxidase homolog gene (accession no: OCC_06611) from *T. litoralis* DSM 5473 in the soluble fraction of *E. coli* BL21 (DE3) using a pET21b vector with a 6X His tag at the C-terminus. We showed that the gene product exhibits L-aspartate oxidase activity in vitro, and this report is the first to detail an L-aspartate oxidase derived from a *Thermococcus* species. The homologs of *Tl*-LASPO distributed mainly in restricted classes of archaea and scarcely in bacteria (Fig. 2). This

Table 4 Kinetic parameters

Temperature (°C)	K_m for L-asp (mM)	V_{max} (µmol/min/mg)	k_{cat} for L-asp (s^{-1})	k_{cat}/K_m (mM^{-1} s^{-1})
37	21.1 ± 5.0	0.82 ± 0.19	0.70 ± 0.16	0.03 ± 0.01
50	14.4 ± 1.7	1.89 ± 0.22	1.61 ± 0.18	0.11 ± 0.02
60	10.2 ± 3.1	2.97 ± 0.90	2.53 ± 0.77	0.25 ± 0.08
70	7.5 ± 1.4	5.00 ± 0.90	4.26 ± 0.77	0.57 ± 0.15

($n = 3$)

might be one of the reasons why the number of report for L-aspartate oxidase purified from bacteria is few in databases for literatures.

The quaternary structure of *Tl*-LASPO was homotrimeric with a subunit molecular mass of 52 kDa. Most of the L-aspartate oxidases reported thus far have been monomeric (Seifert et al. 1990; Marinoni et al. 2008; Bifulco et al. 2013) including the enzyme from *S. tokodaii* strain 7 with the exception of the LASPO from *P. horikoshii* OT-3, which was a homotrimer (Sakuraba et al. 2002). Accordingly, the mechanisms of the thermostabilities of the LASPOs between *Thermococcales* and *Sulfolobus* might be different, but further X-ray crystallographic study must be needed to clarify the relationship between structure and thermostability of *Tl*-LASPO.

When the purified *Tl*-LASPO was stored at 4 °C for more than 96 h, a protein band corresponding to a molecular mass of 100 kDa was detected by SDS-PAGE. This molecular mass (100 kDa) was about twice the subunit molecular mass of *Tl*-LASPO (52 kDa), and the protein band at 100 kDa was probably derived from two polypeptide chains of *Tl*-LASPO. This estimate was supported by the pH dependency of the SDS-PAGE protein band intensity and the total number of free thiol groups (Fig. 3b). The pK_a value of the thiol group of cysteine is generally 6.16, and the H^+ in thiol groups dissociates at alkali pH values. Accordingly, the disulfide bond between two cysteine residues in two polypeptide chains of *Tl*-LASPO might be more easily formed in acidic pH ranges. This observation is specific for *Tl*-LASPO and has not been reported for other LASPOs from hyperthermophilic archaea. A greater number of cysteine residues exist in the primary structure of *Tl*-LASPO (4 cysteine residues: Cys152, Cys351, Cys430, and Cys463) compared with those of LASPOs from *Pyrococcus horikoshii* OT3 (2 cysteine residues) and *Sulfolobus tokodaii* (1 cysteine residues). This reason may explain why *Tl*-LASPO specifically formed a disulfide bond between two polypeptide chains during storage at 4 °C.

Although *Tl*-LASPO activity was highly specific for L-aspartic acid, L-cysteic acid and L-cysteine sulfinic acid also reacted with the enzyme. This substrate specificity of *Tl*-LASPO agreed well with that of the aspartate racemase (EC 5.1.1.13) from *T. litoralis* DSM 5473 (*Tl*-AspR) that we reported in our previous study (Washio et al. 2016). A genome analysis of *T. litoralis* DSM 5473 suggests that L-aspartic acid produced from D-aspartic acid by *Tl*-AspR might be converted to oxaloacetic acid by *Tl*-LASPO. The produced oxaloacetic acid is then probably converted to L-aspartic acid by aspartate aminotransferase, but interestingly, there is no report of aspartate aminotransferase from *T. litoralis* DSM 5473 although 5 putative aspartate aminotransferase genes are annotated in its genome (accession no.: OCC_05516, OCC_03517, OCC_11879, OCC_08839, and OCC_10965). Except aspartate aminotransferase, the putative genes of pyruvate carboxylase subunit B (EC 6.4.1.1; accession no. OCC_09596) and oxaloacetic acid decarboxylase subunit β (EC 4.1.1.3; accession no. OCC_03162) exist in the genome of *T. litoralis* DSM 5473 in relation to oxaloacetic acid metabolism, but these genes seem to encode only a subunit of mature enzymes, and these genes products probably do not function in vivo. Judging from the similarity in substrate specificities in these two enzymes, both D-cysteinic acid and D-cysteine sulfinic acid might convert to sulfopyruvic acid and β-sulfinyl pyruvic acid, respectively, via same enzyme pathway in vivo. The high substrate specificity of *Tl*-LASPO is considered to be useful for the specific conversion of L-aspartic acid to oxaloacetic acid or the quantification of L-aspartic acid in biological samples. Under anaerobic conditions, *Tl*-LASPO utilized fumaric acid, DCIP, and ferricyanide as cofactors in vitro similar to LASPO from *Pyrococcus horikoshii* OT-3 (Sakuraba et al. 2002). These activities are compatible with the enzyme activity of *Tl*-LASPO under aerobic conditions. Since *T. litoralis* DSM 5473 is an anaerobe that grows under only anaerobic conditions, *Tl*-LASPO might catalyze the enzyme reaction in vivo using fumaric acid as a cofactor. The fumaric acid used as a cofactor of *Tl*-LASPO in vivo might be produced from L-aspartic acid via adenylosuccinate by adenylosuccinate synthetase (EC 6.3.4.4; accession no. OCC_02397) and adenylosuccinate lyase (EC 4.3.2.2; accession no. OCC_01109) whose putative genes were encoded in the genome of *T. litoralis* DSM 5473. Interestingly, almost all enzyme gene in tricarboxylic acid (TCA) cycle lacked in the genome of *T. litoralis* DSM 5473 except the putative fumarate hydratase subunit alpha gene (accession no. OCC_11212).

Previous studies on LASPOs in prokaryotes have extensively focused on their role as the first enzyme in the de novo NAD^+ biosynthetic pathway. The homologous genes of this pathway were also conserved in the genome of *T. litoralis* DSM 5473. Accordingly, *Tl*-LASPO might also be related to the NAD^+ biosynthetic pathway in *T. litoralis* DSM 5473, but further studies are needed to clarify the function of *Tl*-LASPO in vivo.

We are currently studying the application of *Tl*-LASPO as an analytical tool for the measurement of L-aspartic acid in various biochemical samples.

Acknowledgements This study was supported in part by the Ministry of Education, Culture, Sports, Science and Technology (MEXT)—Supported Program for the Strategic Research Foundation at Private Universities (Project no. S1311044), 2013–2017.

References

Altschul SF, Gish W, Miller W, Myers EW, Lipman DJ (1990) Basic local alignment search tool. J Mol Biol 215:403–410

Arroyo M, Menendez M, Garcia JL, Campillo N, Hormigo D, de Mata I I, Castillon MP, Acebal C (2007) The role of cofactor

binding in tryptophan accessibility and conformational stability of His-tagged D-amino acid oxidase from *Trigonopsis variabilis*. Biochim Biophys Acta 1774:556–565

Bifulco D, Pollegioni L, Tessaro D, Servi S, Molla G (2013) A thermostable L-aspartate oxidase: a new tool for biotechnological applications. Appl Microbiol Biotechnol 97:7285–7295

Bohmer A, Muller A, Passarge M, Liebs P, Honeck H, Muller HG (1989) A novel L-glutamate oxidase from *Streptomyces endus.* Purification and properties. Eur J Biochem 182:327–332

Braga MD, Martins AM, Amora DN, de Menezes DB, Toyama MH, Toyama DO, Marangoni S, Alves CD, Barbosa PS, de Sousa Alves R, Fonteles MC, Monteiro HS (2008) Purification and biological effects of L-amino acid oxidase isolated from *Bothrops insularis* venom. Toxicon 51:199–207

Flachmann R, Kunz N, Seifert J, Gutlich M, Wientjes FJ, Laufer A, Gassen HG (1988) Molecular biology of pyridine nucleotide biosynthesis in *Escherichia coli.* Cloning and characterization of quinolinate synthesis genes nadA and nadB. Eur J Biochem 175:221–228

Geueke B, Weckbecker A, Hummel W (2007) Overproduction and characterization of a recombinant D-amino acid oxidase from *Arthrobacter protophormiae*. Appl Microbiol Biotechnol 74:1240–1247

Hahn K, Neumeister K, Mix A, Kottke T, Groger H, Fischer von Mollard G (2017) Recombinant expression and characterization of a L-amino acid oxidase from the fungus *Rhizoctonia solani*. Appl Microbiol Biotechnol 101:2853–2864

Isobe K, Sugawara A, Domon H, Fukuta Y, Asano Y (2012) Purification and characterization of an L-amino acid oxidase from *Pseudomonas* sp. AIU 813. J Biosci Bioeng 114:257–261

Katoh A, Uenohara K, Akita M, Hashimoto T (2006) Early steps in the biosynthesis of NAD in *Arabidopsis* start with aspartate and occur in the plastid. Plant Physiol 141:851–857

Leese C, Fotheringham I, Escalettes F, Speight R, Grogan G (2013) Cloning, expression, characterisation and mutational analysis of L-aspartate oxidase from *Pseudomonas putida*. J Mol Catal B 85–86:17–22

Lineweaver H, Burk D (1934) The determination of enzyme dissociation constants. J Am Chem Soc 56:658–666

Marinoni I, Nonnis S, Monteferrante C, Heathcote P, Hartig E, Bottger LH, Trautwein AX, Negri A, Albertini AM, Tedeschi G (2008) Characterization of L-aspartate oxidase and quinolinate synthase from *Bacillus subtilis*. FEBS J 275:5090–5107

Mot YY, Othman I, Sharifah SH (2017) Synergistic antibacterial effect of co-administering adipose-derived mesenchymal stromal cells and *Ophiophagus hannah* L-amino acid oxidase in a mouse model of methicillin-resistant *Staphylococcus aureus*-infected wounds. Stem Cell Res Ther 8:5

Neuner A, Jannasch HW, Belkin S, Stetter KO (1990) *Thermococcus litoralis* sp. nov.: a new species of extremely thermophilic marine archaebacterial. Arch Microbiol 153:205–207

Nishikawa T (2005) Metabolism and functional roles of endogenous D-serine in mammalian brains. Biol Pharm Bull 28:1561–1565

Nishioka M, Mizuguchi H, Fujiwara S, Komatsubara S, Kitabayashi M, Uemura H, Takagi M, Imanaka T (2001) Long and accurate PCR with a mixture of KOD DNA polymerase and its exonuclease deficient mutant enzyme. J Biotechnol 88:141–149

Patsoukis N, Georgiou CD (2004) Determination of the thiol redox state of organisms: new oxidative stress indicators. Anal Bioanal Chem 378:1783–1792

Pilone SM, Pollegioni L, Casalin P, Curti B, Ronchi S (1989) Properties of D-amino-acid oxidase from *Rhodotorula gracilis*. Eur J Biochem 180:199–204

Saitou N, Nei M (1987) The neighbor-joining method: a new method for reconstructing phylogenetic trees. Mol Biol Evol 4:406–425

Sakuraba H, Satomura T, Kawakami R, Yamamoto S, Kawarabayasi Y, Kikuchi H, Ohshima T (2002) L-Aspartate oxidase is present in the anaerobic hyperthermophilic archaeon *Pyrococcus horikoshii* OT-3: characteristics and role in the *de novo* biosynthesis of nicotinamide adenine dinucleotide proposed by genome sequencing. Extremophiles 6:275–281

Sakuraba H, Yoneda K, Asai I, Tsuge H, Katunuma N, Ohshima T (2008) Structure of L-aspartate oxidase from the hyperthermophilic archaeon *Sulfolobus tokodaii*. Biochim Biophys Acta 1784:563–571

Schell MJ, Cooper OB, Snyder SH (1997) D-Aspartate localizations imply neuronal and neuroendocrine roles. Proc Natl Acad Sci USA 94:2013–2018

Seifert J, Kunz N, Flachmann R, Laufer A, Jany KD, Gassen HG (1990) Expression of the *E. coli* nadB gene and characterization of the gene product L-aspartate oxidase. Biol Chem Hoppe Seyler 371:239–248

Stabeli RG, Marcussi S, Carlos GB, Pietro RC, Selistre-de-Araujo HS, Giglio JR, Oliveira EB, Soares AM (2004) Platelet aggregation and antibacterial effects of an L-amino acid oxidase purified from *Bothrops alternatus* snake venom. Bioorg Med Chem 12:2881–2886

Tachibana Y, Takaha T, Fujiwara S, Takagi M, Imanaka T (2000) Acceptor specificity of 4-alpha-glucanotransferase from *Pyrococcus kodakaraensis* KOD1, and synthesis of cycloamylose. J Biosci Bioeng 90:406–409

Takahashi S, Furukawara M, Omae K, Tadokoro N, Saito Y, Abe K, Kera Y (2014) A highly stable D-amino acid oxidase of the thermophilic bacterium *Rubrobacter xylanophilus*. Appl Environ Microbiol 80:7219–7229

Thompson JD, Gibson TJ, Higgins DG (2002) Multiple sequence alignment using ClustalW and ClustalX. Curr Protoc Bioinform Chapter 2, Unit 2.3

Vargas LJ, Quintana JC, Pereanez JA, Nunez V, Sanz L, Calvete J (2013) Cloning and characterization of an antibacterial L-amino acid oxidase from *Crotalus durissus* cumanensis venom. Toxicon 64:1–11

Washio T, Kato S, Oikawa T (2016) Molecular cloning and enzymological characterization of pyridoxal 5′-phosphate independent aspartate racemase from hyperthermophilic archaeon *Thermococcus litoralis* DSM 5473. Extremophiles 20(5):711–721

Wellner D, Meister A (1960) Crystalline L-amino acid oxidase of *Crotalus adamanteus*. J Biol Chem 235:2013–2018